Optics and Detector Improvements for TRINAT’s Time-Reversal Experiment

Michelle Khoo
Co-op 2020S

Supervisor: John Behr, TRINAT

Contents

- Overview of time-reversal experiment:
  - Methods, apparatus, and measurements
- Optics upgrades:
  - 355nm laser replacement
  - Fiber optic selection
- Gamma and positron detection improvements:
  - Energy resolution for varying scintillators and bias voltage
  - Temperature effects on SiPM readout
  - Lightguide geometry optimization
  - Additional considerations (Teflon wrapping, electrical noise, etc.)

Experiment Overview

Magneto-Optical Trap

- TRINAT: “TRIUMF’s Neutral Atom Trap”
- Atoms are confined using a magneto-optical trap (MOT)
  - Three pairs of orthogonal laser beams
  - Quadrupole magnetic field produced by coils

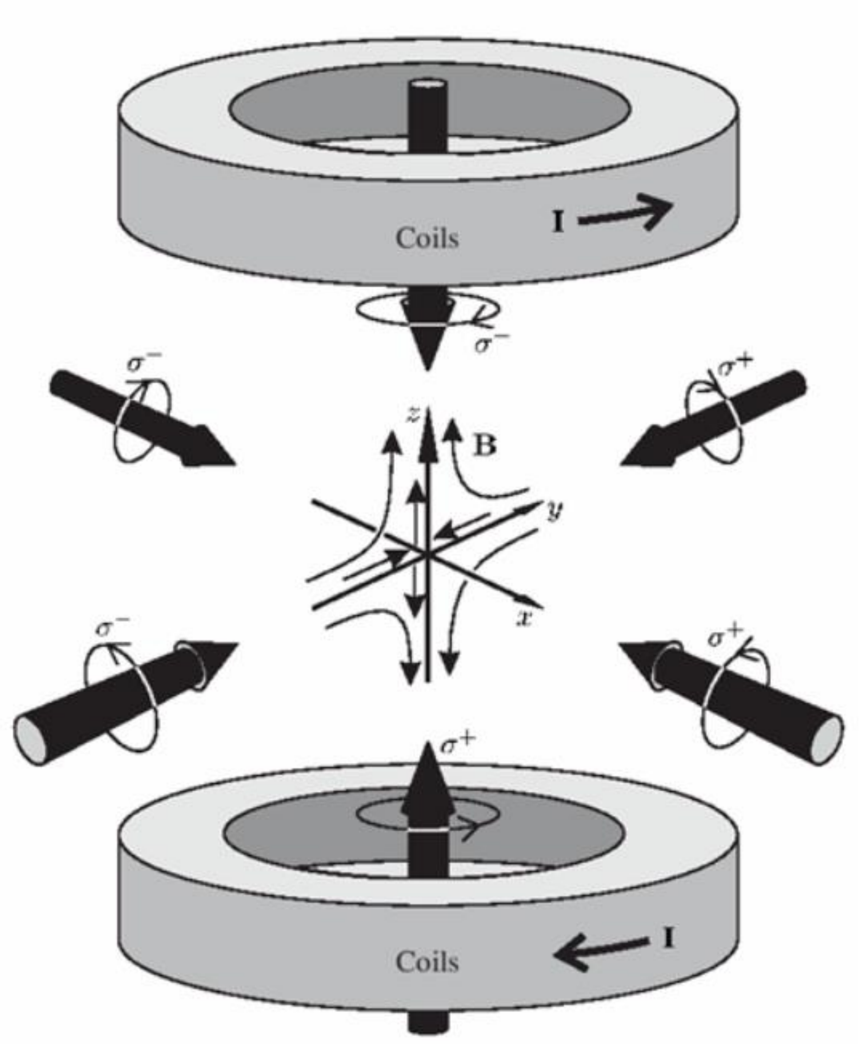

Figure 1: MOT setup (*Atomic Physics,* Foot)

Magneto-Optical Trap (cont’d)

- Orthogonal laser beams are frequency detuned (off-resonance)
  - Moving atoms are Doppler shifted → laser frequency shifted closer to resonance
  - Energy absorption (ie. force) increases as frequency approaches resonance
  - Known as “optical molasses” technique

- Magnetic field produces Zeeman shift
  - Spatially dependent shift in resonant frequency
  - Captures atoms with higher velocities than optical molasses

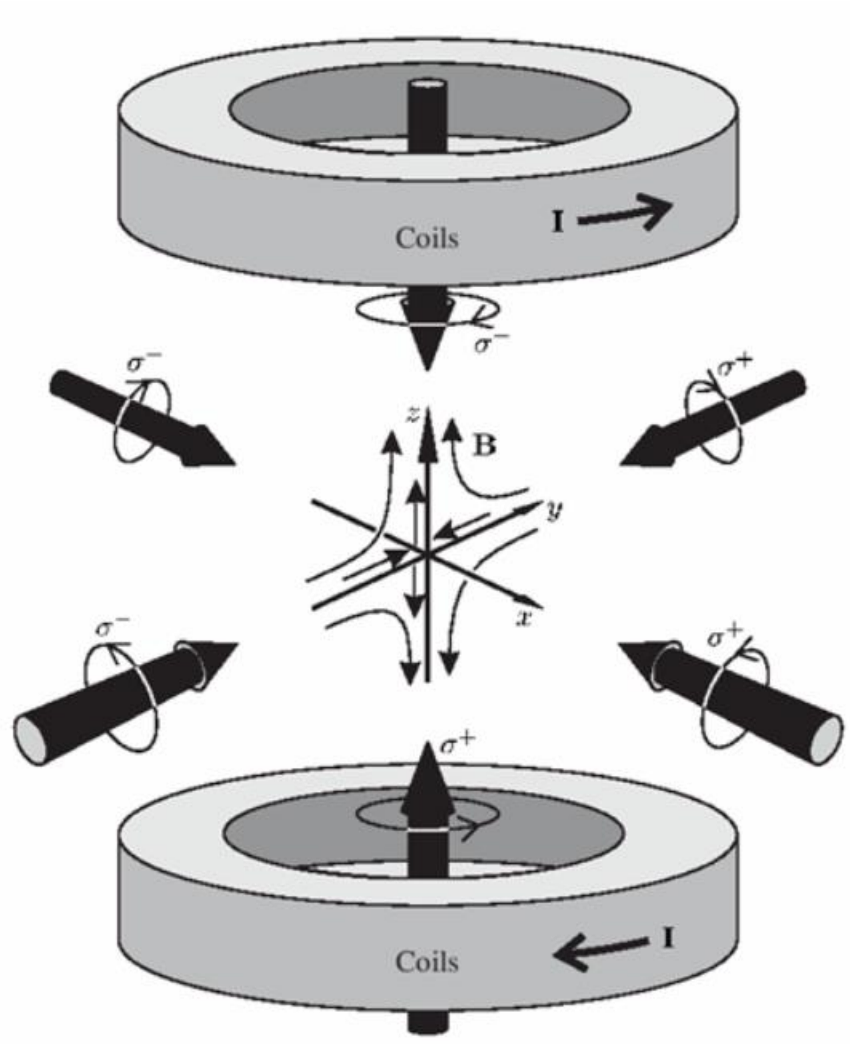

Figure 1: MOT setup (*Atomic Physics,* Foot)

Optical Pumping and Beta Decay

- Trapped atoms are optically pumped by 770nm beam
- Probe polarization by photoionization with 355nm
- Beta-plus decay[1] from ground state of nucleus:

$$37K \rightarrow 37Ar + e^{+} + \nu_e$$

- Decay products detected by scintillators with SiPM[2] readouts (Figure 2)

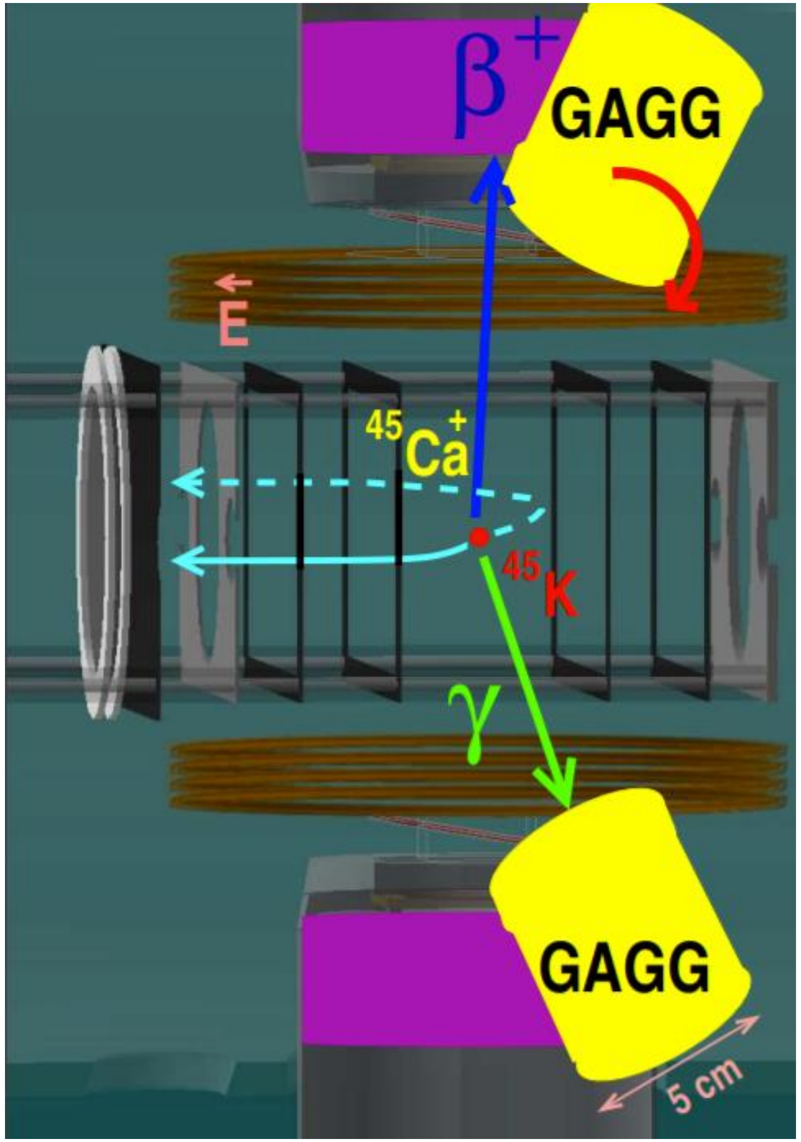

Figure 2: Detector configuration (TRINAT group)

---

[1] Beta-minus decay used for test runs: $45K \rightarrow 45Ca + e^{-} + \bar{\nu}_e$

[2] SiPM: Silicon photomultiplier

Time-Reversal Measurements

- Probe for time-reversal symmetry violation
  - Scalar triple product of momenta ($p1 \cdot p2 \times p3$) always flips sign with time
  - Non-zero average scalar value indicates time-reversal asymmetry

- Three-momentum states always average to zero by momentum conservation
  - Solution: Use a four-momentum state
  - Radiative beta decay has momenta p_{recoil} , p_{β} , p_{ν} , p_{γ}

- Measure beta-neutrino-gamma coincidences: $p_{\beta} \cdot p_{\nu} \times p_{\gamma}$

Optics Upgrades

355nm Laser

- Current setup blocks GAGG detector port
- New setup: CryLaS 355nm laser
  - Couple into polarization-maintaining (PM) single-mode fiber to vacuum chamber
  - Pulse duration (FWHM): 1.00 ns
  - Peak power: 3.5 kW
    → high power risks fiber optic damage

- Benefits of new setup:
  - Doesn't block GAGG port
  - 3x greater power
  - Manual triggering
  - Better mode quality

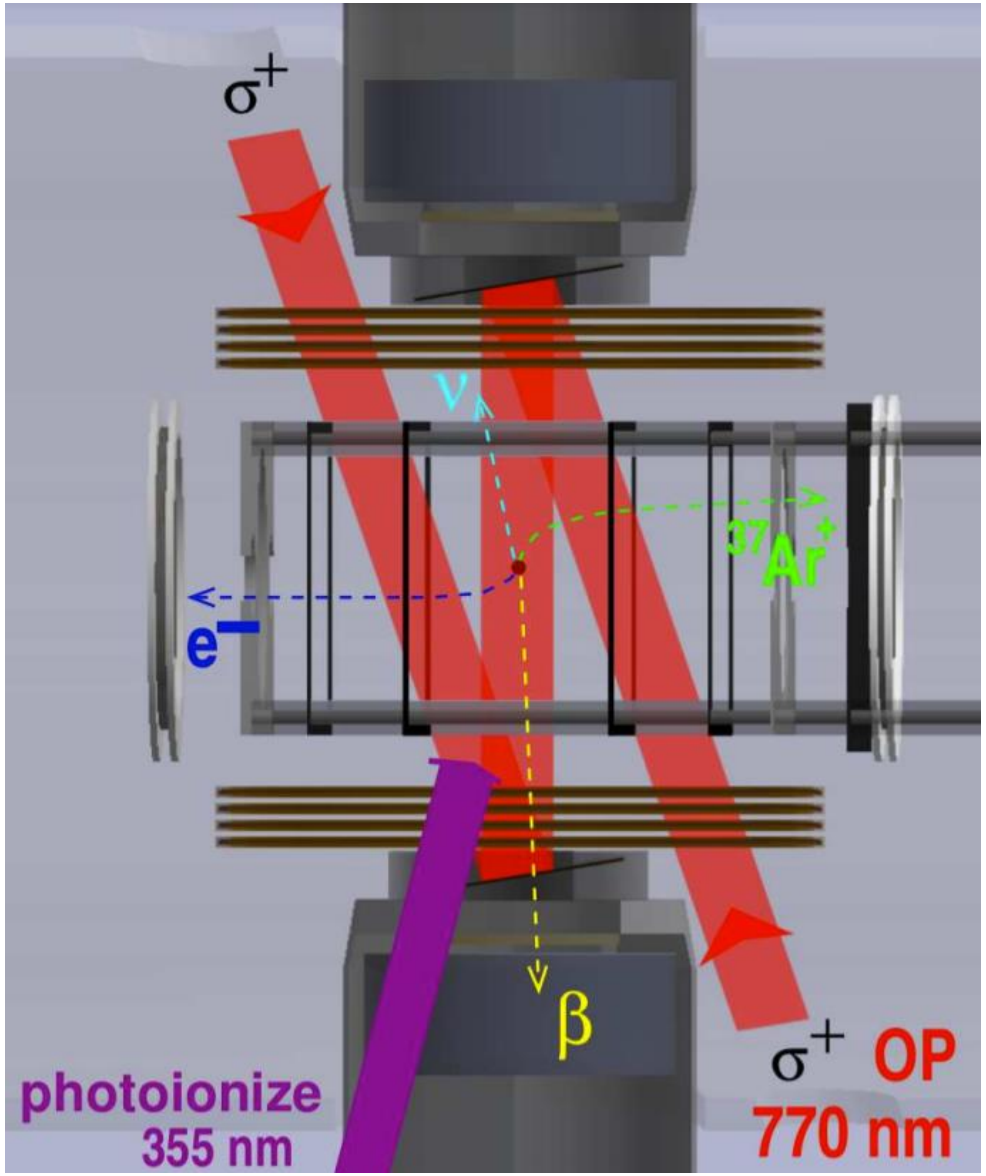

Figure 3: Current optical pumping setup (TRINAT group)

Fiber Optic Constraints

- Power density: Expected power density > laser-induced damage thresholds (LIDT)
  - Single-mode PM fibers have small typical MFD^2 (2.3 um from Thorlabs) → require high LIDT
  - Short pulse duration (1.00 ns) and short wavelength further reduce LIDT
  - Adjusted Thorlabs LIDT: $5\,\frac{GW}{cm^2} * \sqrt{\frac{pulse\ duration}{10\ ns}} * \sqrt{\frac{wavelength}{550\ nm}} \approx 0.25\,\frac{GW}{cm^2}$
  - Expected peak power density: $3.5\ \mathrm{kW} \div \frac{\pi * (2.3\ um)^2}{4} \approx 210\,\frac{GW}{cm^2}$
- Solarization: At UV wavelengths, color centers form within fiber
- Epoxy connectors: At UV wavelengths, epoxy burns and deposits residue (Figure 4)

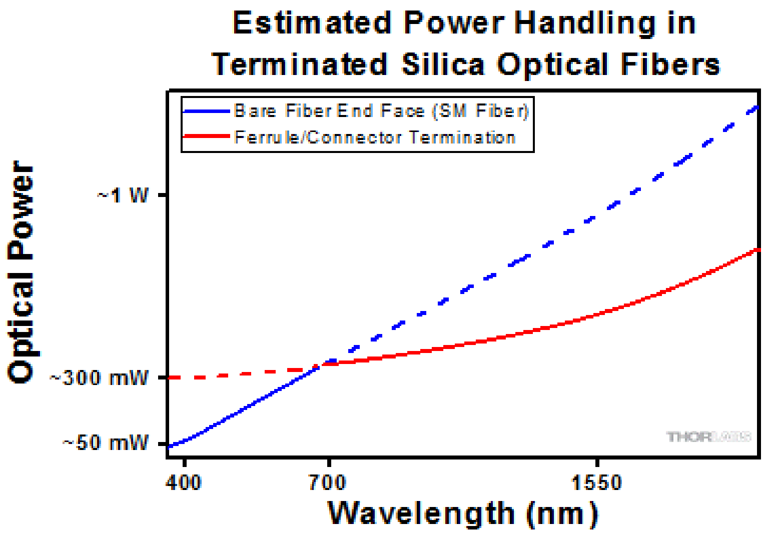

Figure 4: Epoxy damage thresholds (Thorlabs)

---

[3] MFD: Mode field diameter

Fiber Optic Constraints (cont’d)

- Solution:
  - Large-mode area fiber: Increased area reduces power density
  - UV solarization resistant
  - Custom connectors: Minimize epoxy, so that residue is not produced

- Custom fiber is expensive and slow (~3 month lead time)

  → test non-PM fibers
  - Determine impact on mode quality
  - E.g. Newport 320-430 nm single-mode patch cord

Detector Improvements

GAGG Scintillator

- Replaced BGO[4] with GAGG[5] scintillator for gamma ray detection
  - GAGG provides better energy resolution (7.6% from Epic Crystal spec. sheet)

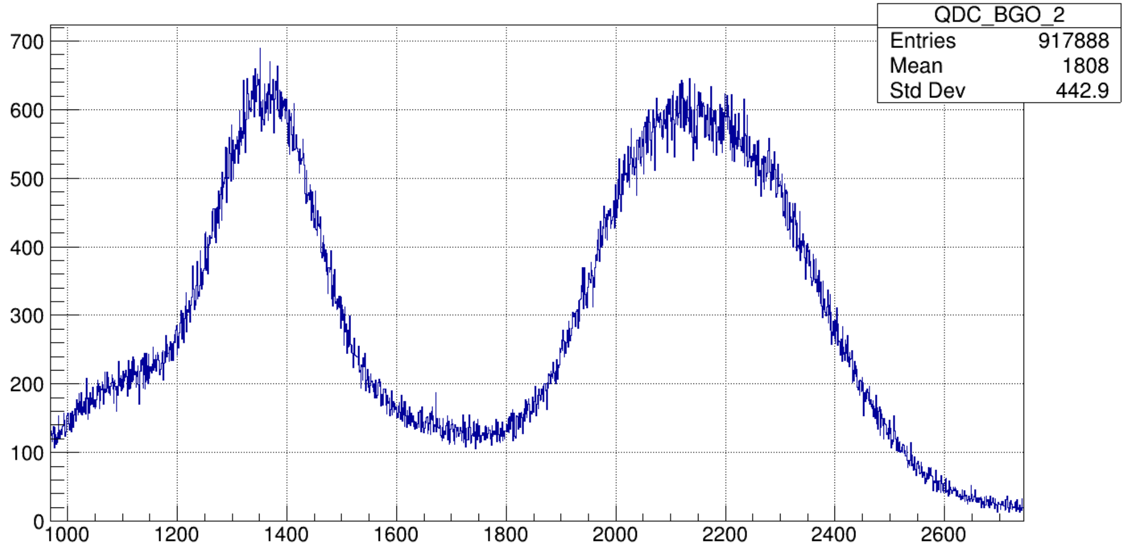

Figure 5: 137Cs and 60Co spectrum with BGO

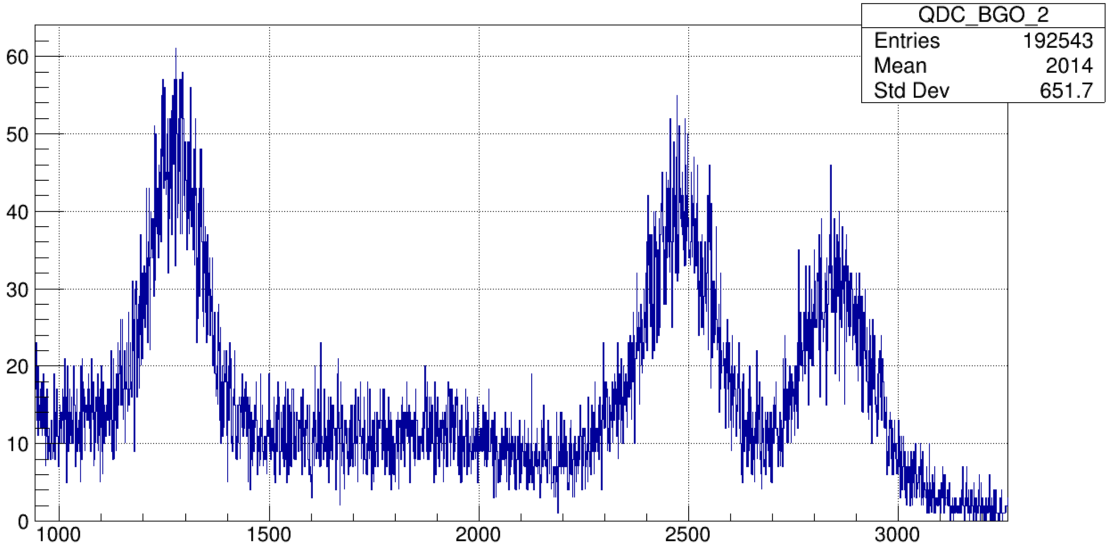

Figure 6: 137Cs and 60Co spectrum with GAGG

---

[4] BGO: Bismuth Germanate

[5] GAGG: Gadolinium Aluminium Gallium Garnet

Bias Voltage Effects

- Increasing overvoltage (Sensl):
    - Increase gain
    - Increase dark current
    - No overall impact on energy resolution (Figure 8)
- **More dark current → lower DC offset (why?)**

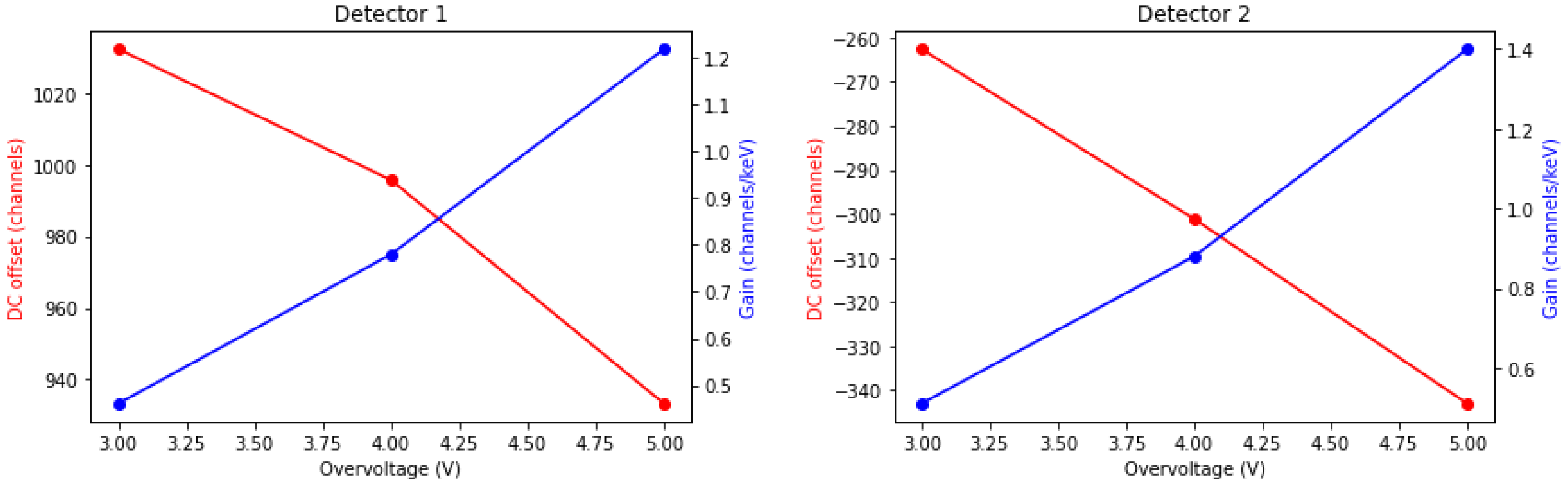

(a)

(b)

Figure 7: DC offset and gain vs. overvoltage for detector 1 (a) and 2 (b)

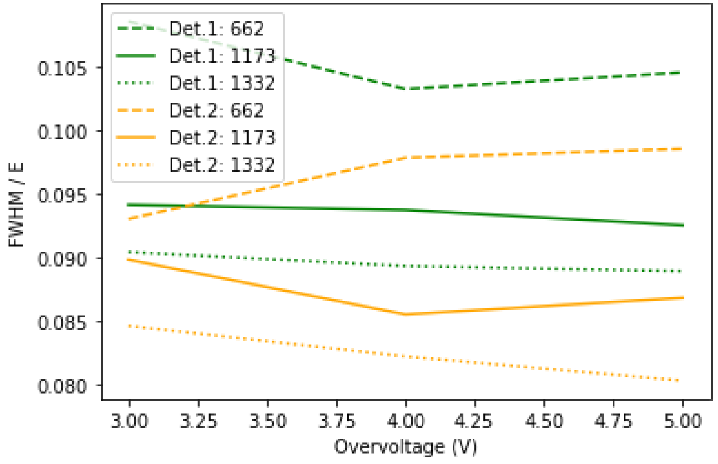

Figure 8: Energy resolution vs. overvoltage

Temperature Effects

- Need a map to convert between histogram channel and gamma energy
  - Plot histogram channel versus energy
  - Use known 137Cs and 60Co peaks (Figure 9)

- DC shift with varying lab temp. due to increased dark current
  - Dark current produced by thermal electrons
  - 50% dark current reduction for every 10°C drop (Sensl)

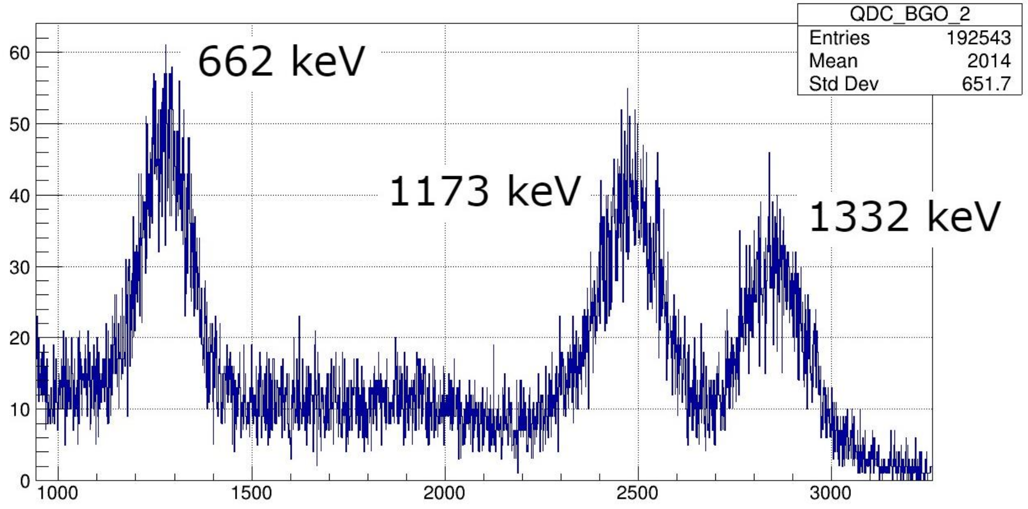

Figure 9: 137Cs and 60Co spectrum with labelled energies

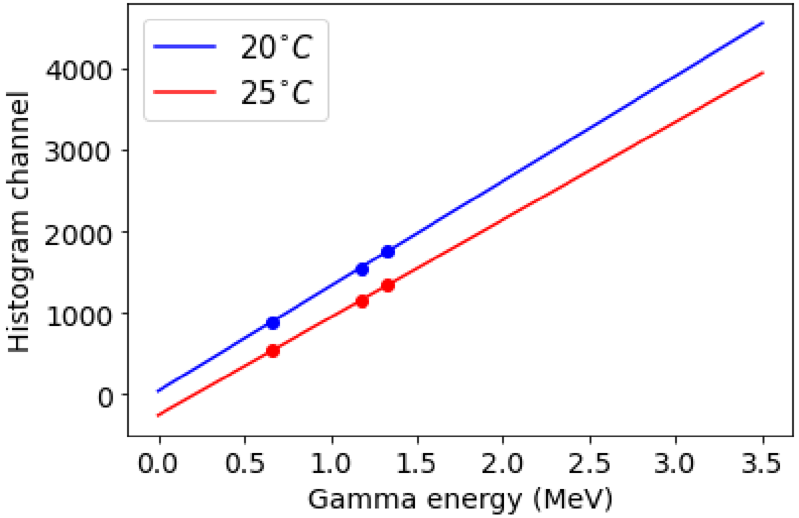

Figure 10: Energy vs. channel at varying lab temperatures

Positron Detector Geometry

- Selected lightguide geometry for a new positron detector, with constraints:
  - Circular face must fit mounting port: ø88 mm
  - Other face must enclose square SiPM array:

    75 mm x 75 mm OR 50 mm x 50 mm

- Options:
  - Expanding lightguide (Figure 11)

    → smaller circle to larger square face

    Narrowing lightguide (Figure 12)

    → larger circle to smaller square face
  - Cylindrical lightguide

    → square SiPM sits within circular face

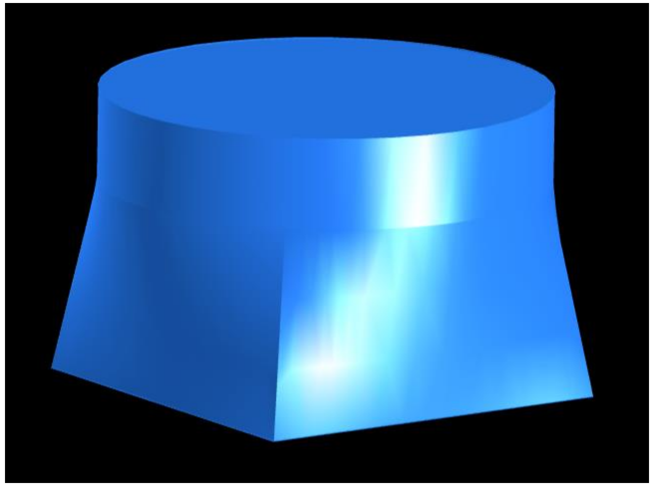

Figure 11: Expanding lightguide

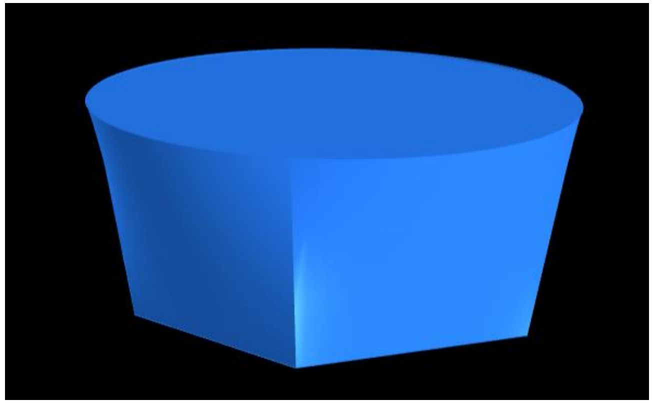

Figure 12: Narrowing lightguide

Positron Detector Geometry (cont'd)

- Selected between geometry options using GEANT4 simulation
  - Modelled lightguide wrapped in Teflon, with a UVT scintillator
  - Counted number of photons that hit the SiPM/square face
  - 100 runs with 5 MeV positrons per geometry option
- Recommend expanding lightguide option

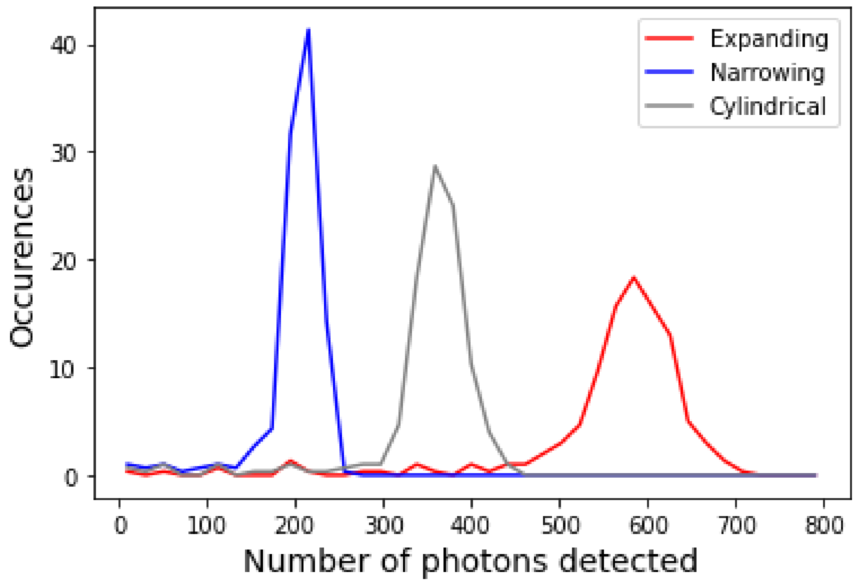

Figure 13: Histogram of photon detection for each geometry

Teflon Wrapping

- Teflon reflectivity has notable impact on light collection, for all geometries (Figure 14)
- Reflectivity is dependent on thickness (Table 1)

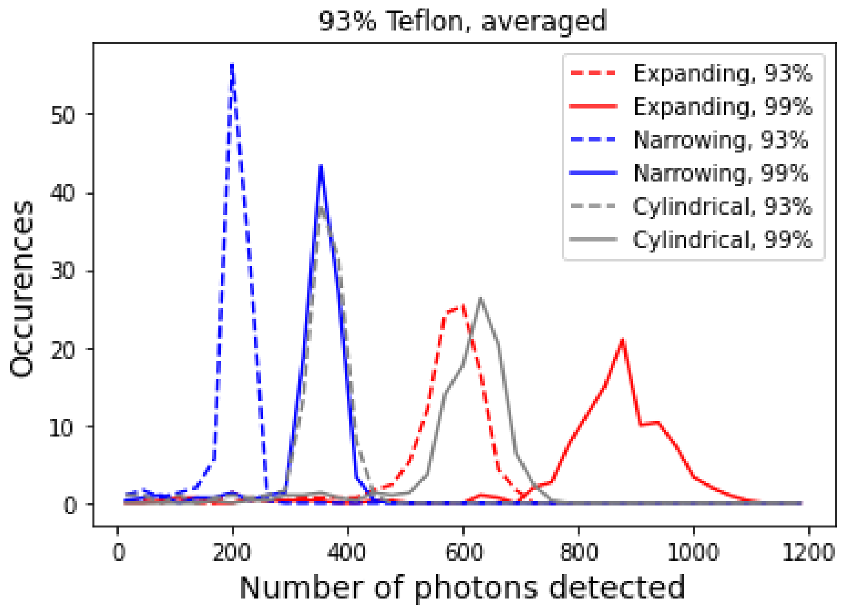

Figure 14: Light collection for varying reflectivity and geometry

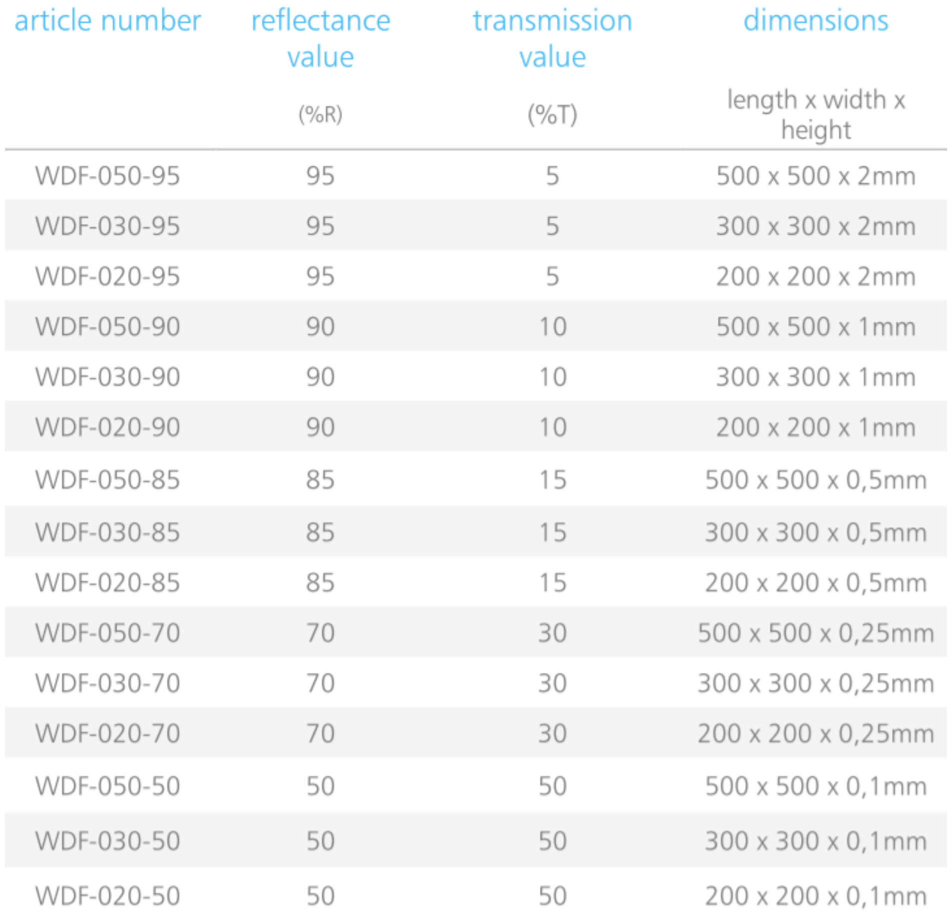

article number	reflectance value (%R)	transmission value (%T)	dimensions length x width x height
WDF-050-95	95	5	500 x 500 x 2mm
WDF-030-95	95	5	300 x 300 x 2mm
WDF-020-95	95	5	200 x 200 x 2mm
WDF-050-90	90	10	500 x 500 x 1mm
WDF-030-90	90	10	300 x 300 x 1mm
WDF-020-90	90	10	200 x 200 x 1mm
WDF-050-85	85	15	500 x 500 x 0,5mm
WDF-030-85	85	15	300 x 300 x 0,5mm
WDF-020-85	85	15	200 x 200 x 0,5mm
WDF-050-70	70	30	500 x 500 x 0,25mm
WDF-030-70	70	30	300 x 300 x 0,25mm
WDF-020-70	70	30	200 x 200 x 0,25mm
WDF-050-50	50	50	500 x 500 x 0,1mm
WDF-030-50	50	50	300 x 300 x 0,1mm
WDF-020-50	50	50	200 x 200 x 0,1mm

Table 1: Teflon reflectivity for various dimensions (Spectralex)

Additional Improvements

- Found significant 10 MHz noise in SiPM readout

- Electrical considerations:
  - Currently using standard BNCs → replace with two-pin LEMO
  - Improve grounding scheme to reduce ground loops

- Other considerations:
  - Identify noise source and build shielding

Summary

Recent/Upcoming upgrades to TRINAT’s optics include:

- Replacement 355 nm photoionizing beam
- Fiber optic coupling into chamber

In order to optimize TRINAT’s detectors, consider:

- Scintillator selection, lightguide geometry, and Teflon thickness significantly impact performance
- Temperature effects need to be accounted for when mapping histogram channels to gamma energy
- Improved grounding and shielding may reduce external noise pickup

These considerations are expected to improve precision measurements for beamtime in Fall/Winter 2021.